EUROPEAN ORGANIZATION FOR NUCLEAR RESEARCH
European Laboratory for Particle Physics

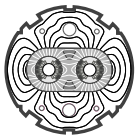

Large Hadron Collider Project

LHC Project Report 136

Numerical Evaluation of Long-term Stability

M. GIOVANNOZZI* W. SCANDALE† E. TODESCO*

Abstract

The problem of predicting long-term particle loss in 4D betatronic motion is considered. A phenomenological scenario is derived through numerical tools based on tracking and frequency analysis. A three-parameter formula to interpolate the dynamic aperture versus the number of turns is proposed. The agreement with tracking data is excellent, and the extrapolation for very high number of turns agrees with the onset of chaos evaluated through the Lyapunov method.

*Dipartimento di Fisica, Universitá di Bologna, Via Irnerio 46, 40126 Bologna Italy
†CERN, SL Division, CH 1211 Geneve Switzerland

Submitted at the Workshop on 'New Ideas for Particle Accelerators', S. Barbara, Ca, USA, November 1996

Administrative Secretariat
LHC Division
CERN
CH-1211 Geneva 23
Switzerland

Geneva, 9 September 1997

Introduction

Modern hadron colliders based on superconducting magnets suffer from the unavidable effect of field-shape distortions, particularly harmfull during the injection plateau. This critical period can last a considerable number of turn making difficult to evaluate the single-particle stability with computer tracking simulations. For instance, in the case of the CERN Large Hadron Collider [1] the injection process will last of the order of 10^7 turns. On the other hand, numerical simulations based on symplectic tracking can hardly reach $10^5 - 10^6$ turns. In addition, a dense sampling of the phase space is crucial to obtain significant results from numerical tracking. Three main approaches have been proposed in the past to speed-up the investigations on beam stability: the determination of the onset of chaotic behaviour using the maximal Lyapunov exponent [2, 3], the evaluation of the drift in the space of approximated invariants carefully evaluated through numerical methods [4], and the visualization of the dynamic aperture reduction with increasing number of turns through survival plots [6, 7].

In this paper we investigate in an extensive manner the last one using a simplified model of 4D betatronic motion where the coupling with longitudinal dynamics and the modulation of the linear frequencies are neglected. We propose some numerical tools and we derive a phenomenological scenario to interpret the results of our simulations. We recall a way to define the dynamic aperture [14] and we show how it can be interpolated using a three-parameter formula that can be interpreted in terms of the Nekhoroshev and KAM theorem. The interpolation fits very well with the numerical data and agrees with the prediction of the onset of chaos provided by the Lyapunov exponent. Additional studies to check the validity of this scenario in a more realistic accelerator model, describing 6D motion and includind the ripple effect, are in progress [8, 9].

Models

In this paper we restrict ourselves to the analysis of the betatron motion neglecting the effect of coupling with the synchrotron motion. Therefore, the map that simulates the single-particle dynamics over one turn of the machine has a four dimensional phase space, and its linear part is the direct product of two rotations of frequencies ω_1 and ω_2. A prototype of these models is the Hénon map that represents a linear lattice with a sextupole in the one-kick approximation:

$$\begin{pmatrix} x' \\ p'_x \\ y' \\ p'_y \end{pmatrix} = \begin{pmatrix} R(\omega_1) & 0 \\ 0 & R(\omega_1) \end{pmatrix} \begin{pmatrix} x \\ p_x + x^2 - y^2 \\ y \\ p_y - 2xy \end{pmatrix}. \tag{1}$$

We made several simulations of this model for different values of the linear frequencies. In this paper we will only present the results relative to this model. Simulations over a 4D model of the LHC have confirmed the results obtained for the Hénon map [3].

Analysis of the phase space

In this section we review some numerical tools based on frequency analysis [3, 10, 11, 12] to determine the position and the width of resonances in the 4D phase space. We consider a grid of initial conditions on the plane (x, y), $p_x = p_y = 0$. The numerical

method is based on two tools: the orbit of length N associated to each initial condition is evaluated through the iteration of the map, and then the main frequencies are computed using an interpolation of the FFT plus Hanning filter [12]. This methods provides under some general conditions a precision of the order of $1/N^4$ for regular trajectories (where the frequencies are well defined). For chaotic orbits the frequencies are not defined and the algorithm provides quantities that can considerably vary along the discrete time N, and that do not converge for $N \to \infty$.

For each intial condition, the simulations provide the number of turns n up to which the particle is stable and the two nonlinear frequencies (ν_1, ν_2). One can display this information through the following plots:

- long-term plot: each initial condition (x, y) is plotted using a different marker according to the number of turns n where particle loss occurs. One can visualize the shape of the dynamic aperture and how it shrinks when the length of the orbit N increases;
- tune footprint (or image of the frequency map): the frequencies are plotted in the frequency space. This provides very relevant information about what part of the tune diagram is covered by the stable initial conditions. Moreover, depletion regions around resonance lines indicate that the resonance is excited since there is a strong phase locking;
- network of resonances: only the initial conditions that are locked on resonances, i.e. whose frequencies satisfy

$$q\nu_1 + p\nu_2 = l + \epsilon \qquad\qquad q, p, l \in \mathbf{Z} \tag{2}$$

  are plotted in the coordinate plane (x, y). We used 2048 iterates and $\epsilon = 10^{-4}$. This plot provides very relevant information since it directly displays the size of resonances, their position in phase space, and their relation with the dynamic aperture. Contrary to the tune footprint, this plot is not invariant under the selection of the initial phases. Nevertheless the plot is invariant under the linear dynamics and therefore a change in the initial phases does not significantly affect the pattern obtained, leading only to some deformations at high amplitudes. Indeed, one can produce similar plots in the space of the nonlinear invariants [13] by evaluating them through numerical methods. In this way one can rigorously measure the position of the resonances and their width in phase space. We will not use this method since we are interested only in a qualitative analysis of the phase space dynamics.

In Fig. 1 we show a very dense long-term plot for the Hénon map [see Eq. (1)] with linear frequencies $\nu_x = 0.168$, $\nu_y = 0.201$. A rectangular grid of 250×250 initial conditions is iterated for 10^8 turns. The different shadows of grey correspond to the particle loss number. It turns out that one has an inner region where all the particle are stable for at least 10^8 turns; such a region features no holes with the used resolution in the initial conditions scan. Then, one finds a rather irregular but sharp border of instability: outside the border, one has a chaotic sea of initial conditions that are lost between 10^8 and $10^3 - 10^2$ turns; no structure is visible in this region, and neighbour initial conditions can be lost at number of turns n that may differ by one or two orders of magnitude. Finally, there is an outer region of fast particle loss ($10 - 10^2$ turns) where the dependence of the initial conditions on n is much smoother, and some structures probably associated with hyperbolic manifolds are visible.

In Fig. 2 we show the network of resonances of the same model. One finds very large resonances that are stable; moreover, the mechanism of particle loss due to the

diffusion along the resonant channels or due to resonance crossing does not seem to be very relevant. Indeed, the bulk of long-term losses occur in the wide chaotic band where no resonance structures are visible. This chaotic band is characterized by isolated points locked on very low order resonances, that appear in the figure as a set of scattered dots. The same analysis has been carried out for other models, and also for a 4D model of the LHC [3], leading to the same qualitative results. In Figs. 3 and 4 we show the long-term plot and the resonance network for the Hénon map with linear frequencies $\nu_x = 0.201$, $\nu_y = 0.112$. Also in this case most long-term losses occur in the wide chaotic band localized at $x \in [0.25, 0.45]$, $y \in [0.0.3]$ that can be recognized in the resonance network by the presence of isolated initial conditions locked on low-order resonances. Moreover, in this case one has the rather striking presence of a very large resonance that is stable for at least 10^7 turns. The size of this resonance cannot be evaluated by analyzing the tune

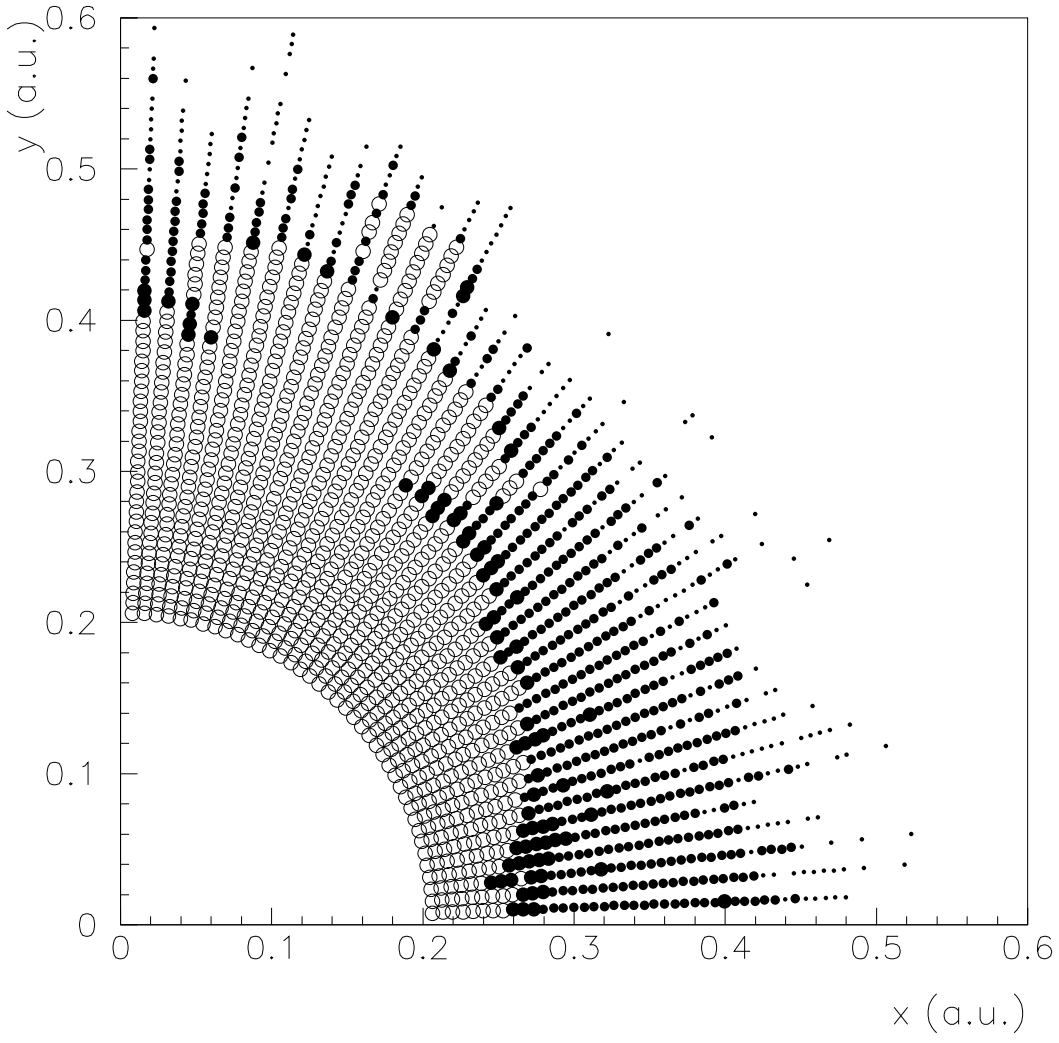

Figure 1: Long-term plot of the Hènon map at $\nu_x = 0.168$, $\nu_y = 0.201$: black dots represent initial conditions stable up to 10^8 turns; shadows of grey represent unstable initial conditions (lighter grey corresponds to shorter stability time).

footprint, that only displays a strong phase locking around that resonance.

The conclusions of this qualitative analysis are the following:

- there is a rather sharp border that separates stable from unstable initial conditions for the considered number of turns ($10^7 - 10^8$);
- long-term particle losses mainly occur in wide chaotic bands where all the integrable structure has been wiped out;
- the mechanism of diffusion along the resonant channels and due to resonance crossing are rather weak.

Dynamic Aperture and Associated Errors

In a previous work [14] we have proposed a definition of dynamic aperture as a function of the number of turns N as the first amplitude where particle loss occurs before N turns, averaged over the phase space. Particles are started along a 2D polar grid in the coordinate space (x, y):

$$x = r\cos\theta \qquad\qquad y = r\sin\theta \tag{3}$$

and the intial momenta p_x p_y are set to zero. Let $r(\theta; N)$ be the last stable initial condition along θ before the first loss at a turn number lower than N occurs. Then the dynamic aperture is defined as

$$D = \left(\int_0^{\pi/2} [r(\theta; N)]^4 \sin 2\theta d\theta\right)^{1/4}. \tag{4}$$

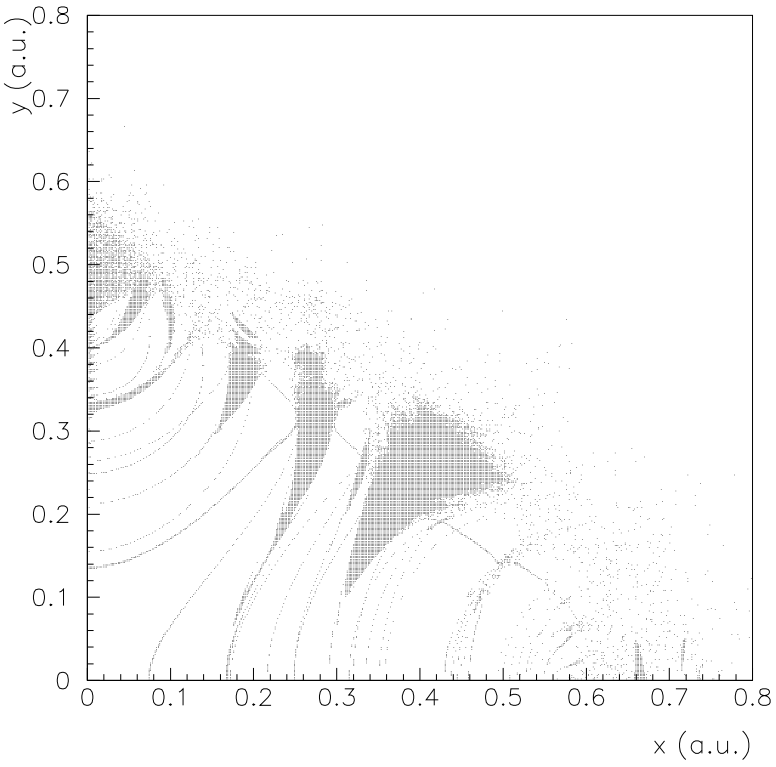

Figure 2: Network of resonances of the Hènon map at $\nu_x = 0.168$, $\nu_y = 0.201$: black dots represent initial conditions locked on resonances up to order 15.

With respect to the approach used in several long-term simulations (see for instance [6, 7]), where the scan over only one variable is considered in order to speed up simulations, this definition provides a smoother dependence of D on N, thus allowing to derive interpolating formulas and to extrapolate them to predict long-term particle loss.

One of the crucial issues in the definition of the dynamic aperture is the determination of the error associated to the estimate in computer simulations. When definition (4) is implemented one has to carry out two discretizations: one over the radial variable r and one over the angular variable θ. Let $\Delta r = (r_{max} - r_{min})/N_r$ and $\Delta\theta = \pi/2N_\theta$ be the step size in r and θ respectively. The total error can be obtained using gaussian sum in quadrature

$$\Delta D = \sqrt{\left(\frac{\partial D}{\partial r}\frac{\Delta r}{2}\right)^2 + \left(\frac{\partial D}{\partial \theta}\frac{\Delta \theta}{2}\right)^2}. \tag{5}$$

An approximated formula for the error can be obtained by replacing the dynamic aperture definition with a simple average over θ

$$D = \frac{2}{\pi}\int_0^{\pi/2} r(\theta; N) d\theta \equiv < r(\theta; N) > . \tag{6}$$

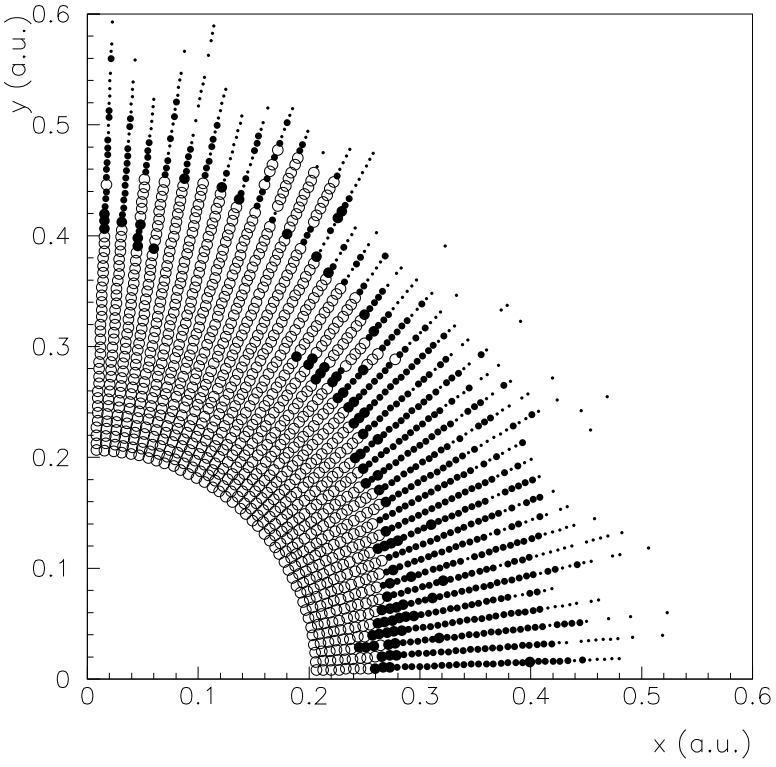

Figure 3: Long-term plot of the Hènon map at $\nu_x = 0.201$, $\nu_y = 0.112$: empty circles represent initial conditions stable up to 10^7 turns; full circles represent unstable initial conditions (smaller circles correspond to shorter stability times).

Using this formula the associated error reads

$$\Delta D = \sqrt{\frac{(\Delta r)^2}{4} + < |\frac{\partial r}{\partial \theta}| >^2 \frac{(\Delta \theta)^2}{4}} \tag{7}$$

and therefore it turns out that the step in r must be equal to the step in θ times $< |\frac{\partial r}{\partial \theta}| >$ in order to have an optimization of the integration steps.

Prediction based on Lyapunov Exponent

A method that has been used to select chaotic from regular orbits in nonlinear dynamical systems is based on the evaluation of the maximal Lyapunov exponent [2, 3, 15, 16, 17]. For a given initial condition, the Lyapunov $\lambda(N)$ is evaluated using an orbit of N turns. The theory states that if $\lim_{N\to\infty} \lambda(N) = 0$, the orbit is regular and therefore the particle is stable; on the other hand, if the limit is positive, then the particle is chaotic (i.e., there is sensitivity to initial conditions and exponential divergence of neighbour trajectories), and therefore it can be lost. The Lyapunov method allows one to determine the border between chaotic and regular motion. On the other hand, it does not give information about how this limit is reached when N tends to infinity.

In Ref. [3] we have proposed an automatic method to select regular from chaotic orbits based on a threshold on the Lyapunov. Since for regular particles the distance between neighbour orbits linearly increases with the discrete time N, one can fix a threshold

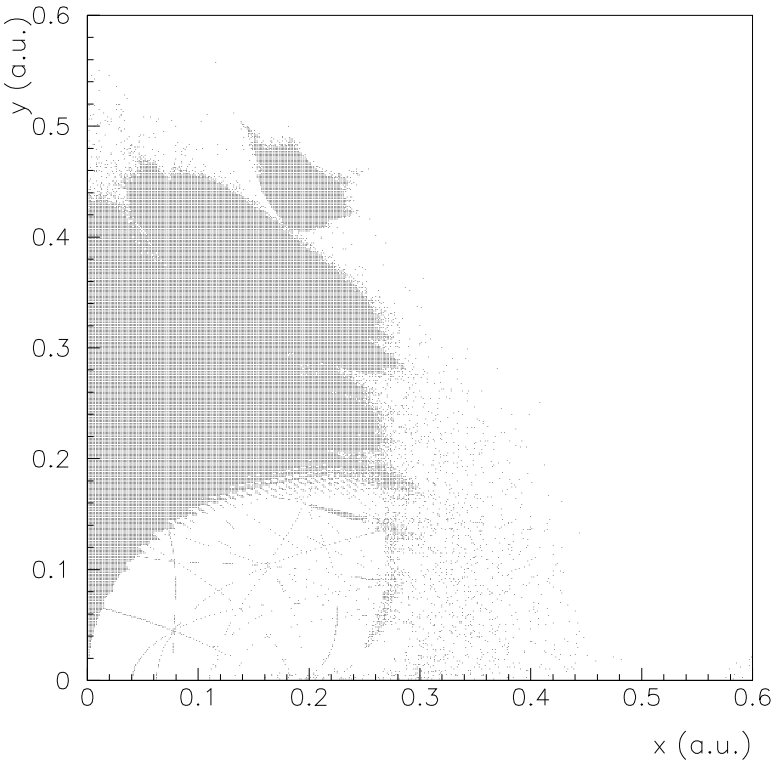

Figure 4: Network of resonances of the Hènon map at $\nu_x = 0.201$, $\nu_y = 0.112$: black dots represent initial conditions locked on resonances up to order 15.

according to

$$\sigma_\lambda(N) = \frac{1}{N} \log A_\lambda N \tag{8}$$

If $\lambda(N) > \sigma_\lambda(N)$, then the particle is assumed to be chaotic, whilst if $\lambda(N) < \sigma_\lambda(N)$ the particle is regular. The thresholds $\sigma_\lambda(N)$ can be determined by the analysis of the distribution of the Lyapunov evaluated at N turns for the chosen set of initial conditions. We refer to Ref. [3] for more details. It turns out that the thresholds are very well interpolated by Eq. (8), and that the constant A_λ seems to depend very weakly on the model. In fact, we found for all our simulations (Hénon, SPS, LHC 4D, LHC 6D, see Ref. [3]) the value $A_\lambda = 0.5$.

Prediction based on Extrapolation

During the past years, extensive tracking has been carried out to determine the long-term stability of both existing and planned machines. A very effective way to display the tracking data is provided by survival plots[6, 7], where the particle loss number n is plotted versus the initial amplitude A for a given lattice. The obtained pattern is in general rather irregular; in fact, due to the complicated structure of the chaotic region (see the previous sections), the dependence of n versus the amplitude is far from being regular. Therefore, an extrapolation to a larger number of turns is very hard to obtain. The definition of dynamic aperture given in the previous section allows one to make the survival plot considerably smoother, and therefore an interpolation becomes possible. In Fig. 5 we show $D(N)$ versus N for the same model of Fig. 1, carrying out simulations up to 10^8 turns. A very fine phase space scan (120 radial steps from 0.3 to 0.8 and 60 angular step) has been used in order to obtain a very small error (of the order of 1%).

In Ref. [3] we have proposed an "inverse log" behaviour to interpolate the dynamic aperture:

$$D(N) = D_\infty \left(1 + \frac{b}{\log N}\right). \tag{9}$$

An heuristic interpretation of this formula has been proposed [18] according to two main theorems of dynamical systems, namely KAM [19] and Nekhoroshev [20, 21, 22, 23] theorems. One assumes that the phase space is divided into two regimes:

- an inner region where almost all the phase space is foliated into KAM tori, except a very small fraction where the Arnold diffusion can take place over the resonance web. This region appears in simulations as a "full" domain of initial conditions stable for extremely high number of turns;
- an outer region where almost all the foliation of phase space in KAM tori has been destroyed, and only a wide chaotic sea is left. Since we are close to the last KAM tori, we assume that in this region the particles escape to infinity with the rate provided by the Nekhoroshev estimate:

$$N(r) = N_0 \exp\left(\frac{r_*}{r}\right)^{1/\kappa}, \tag{10}$$

where $N(r)$ is the number of turns that are estimated to be stable for particles with initial amplitude smaller than r. The inversion of the above formula provides

$$r(N) = \frac{r_*}{\log^\kappa(N/N_0)}. \tag{11}$$

In order to check out this scenario, we have carried out the following simulations over the model used in Fig. 1: we choose initial conditions along $x = y = A$ and $p_x = p_y = 0$, and for each amplitude A we start a dense cloud of initial conditions around A (1000 particles with a neighbourhood size of 10^{-4}). We compute the fraction $S(A;N)$ of the particles that are stable for at least N turns: assuming that all the chaotic particles are unstable, the $\lim_{N\to\infty} S(A;N)$ is the local fraction $S(A)$ of the phase space foliated into invariant tori as a function of the amplitude. If the proposed scenario is valid, one should find a good approximation of the theta function, i.e. $S(A)$ should be very close to one for $A < A_\infty$, and then it should fall abruptly to zero. The results shown in Fig. 6 for $S(A;10^7)$ fully confirm this scenario: the phase space region where one has comparable probability of finding both KAM tori and chaotic regions seems to be very small. Moreover, for $A < A_\infty$, $S(A;10^7)$ is exactly equal to one, i.e. for each A all the 10^3 particles were found to be stable. This confirms that the Arnold diffusion for this kind of models is extremely weak and therefore is not an important mechanism for the determination of the dynamic aperture.

Adding the information obtained from the KAM theorem (the existence of a positive D_∞) and from the Nekhoroshev theorem (the inverse log decaying of the dynamic aperture), one obtains the following equation

$$D(N) = D_\infty \left(1 + \frac{b}{\log^\kappa(N/N_0)}\right) \tag{12}$$

that reduces to Eq. 9 for $N_0 = \kappa = 1$. We tried to interpolate the data shown in Fig. 5

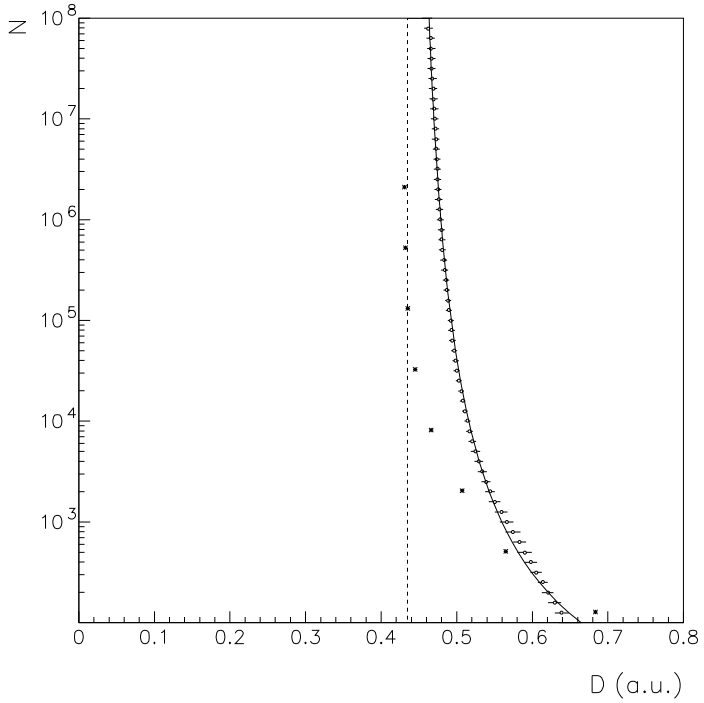

Figure 5: Dynamic aperture versus number of turns (dots) for the Hènon map at $\nu_x = 0.168$, $\nu_y = 0.201$; analytic interpolation (solid line) and extrapolation at infinity (dotted line). Prediction of the chaotic border according to the Lyapunov exponent (stars).

with this formula using three free parameters D_∞, b and the exponent κ. We fixed N_0 to one by using the heuristic argument that $D(1) = \infty$. In order to find a solution, we made a scan over κ and for each κ we evaluated D_∞, and b by solving a linear system. Then we computed the χ^2 function, i.e.

$$\chi^2 = \frac{1}{J-3} \sum_{j=1}^{J} \frac{(D(N_j) - \hat{D}(N_j))^2}{\sigma_i} \tag{13}$$

where the interpolated dynamic aperture $\hat{D}(N_i)$ according to Eq. (9) is evaluated at the turn number N_i, and $\sqrt{\sigma_i}$ is the error estimated through Eq. (7). It turns out that:

- it is rather difficult to determine the exponent with a high precision. For instance, if we consider all the exponents that provide a χ smaller than 0.7, that corresponds in our case of a confidence level of 95%, we obtain $\kappa \in [0.9, 2]$;
- the optimal exponent for our case turns out to be around 1.5. The interpolation is shown in Fig. 5 as a solid line, and agrees very well with tracking data. The theory of Nekhoroshev for mappings [23, 22] provides an estimate for the exponent κ that is equal to the number of degrees of freedom plus one, i.e. in our case $\kappa = 3$. This value of κ does not agree with our simulations. Indeed, a refined version of the theorem [24] leads to the improved estimate $\kappa = (1+d)/2$, i.e. in our case $\kappa = 1.5$. This is in agreement with our simulations; additional checks for higher dimensions would be highly desirable in order to cross-check the optimal estimate of the exponent with the validity of our scenario.

We have also computed the estimate of the chaotic border through the Lyapunov exponent, using the same type of definition for the dynamic aperture, where now $r(\theta)$ the amplitude of the particle immediately before the first particle along θ whose Lyapunov is greater than the threshold. In Fig. 5 we show, together with the tracking data and with

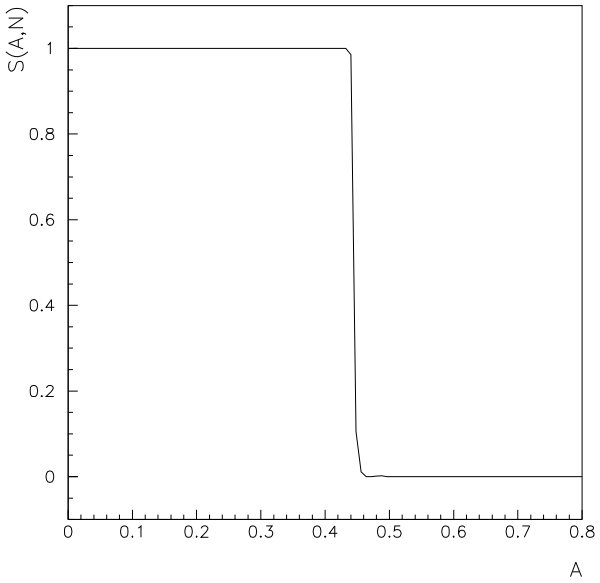

Figure 6: Fraction of the particles stable for 10^7 turns around the initial condition $x = y = A$, $p_x = p_y = 0$ for the Hènon map at $\nu_x = 0.168$, $\nu_y = 0.201$.

the interpolation, the guess provided by the Lyapunov exponent at increasing number of turns. It turns out that the Lyapunov guess of the chaotic border seems to approach rather rapidly (when compared to tracking) the dynamic aperture value extrapolated to infinity according to our formula. This result confirms the scenario illustrated in the previous section. The same simulations have been carried out for two other Hénon maps with different linear frequencies. The dynamic aperture data, the interpolation and the Lyapunov prediction are shown in Fig. 7 and 8. The results fully agree with the scenario described for the previous case.

Conclusion

We have analysed simplified models of the 4D betatronic motion to derive a phenomenological description of the mechanisms of instability and to build numerical methods to predict long-term particle loss. Long-term tracking of very dense sets of initial conditions shows that particle loss mainly occurs in macroscopic chaotic bands. Other mechanisms such as Arnold diffusion or diffusion along resonances are shown to be rather weak. We also show that the dynamic aperture, computed as an average over the ratio of emittances, is very well interpolated by an empirical law that can be justified in terms of KAM and Nekhoroshev theorem. The determination of the exponent in the inverse log formula is affected by a rather large error, but the extrapolation is reliable. Moreover, the extrapolation for infinite number of turns agrees well with the guess provided by the Lyapunov method. Even though relevant studies for the 6D case have been already carried out [2, 3, 8], we believe that additional analysis should be done, including also the ripple

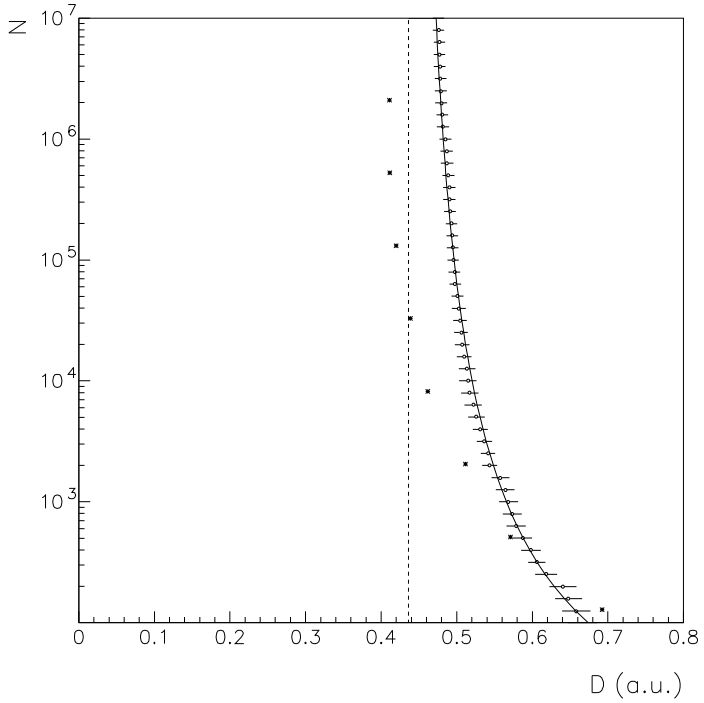

Figure 7: Dynamic aperture versus number of turns (dots) for the Hènon map at $\nu_x = 0.201$, $\nu_y = 0.168$; analytic interpolation (solid line) and extrapolation at infinity (dotted line). Prediction of the chaotic border according to the Lyapunov exponent (stars).

effect, in order to see how the presence of an additional degree of freedom modifies the proposed scenario and the predictivity of the numerical tools.

Acknowledgements

We wish to thank Prof. Turchetti for very relevant contributions to the analysis and to the interpretation of the tracking data. Special thanks to S. Bongini, M. Böge, J. Ellison, J. Irwin, F. Schmidt and B. Warnock, for constructive discussions. E. Todesco would like to thank Z. Parsa and G. Guignard for the invitation to the program, the ITP staff for the very effective organization of the workshop, Anu Venugopalan, Vera and Raymond Holgate, and the management of "L'Agave" for the warm welcome to S. Barbara.

References

[1] The LHC Study Group, *CERN–LHC* **95-05** (1995).
[2] Schmidt, F., Willeke, F., and Zimmermann, F. , *Part. Accel.* **35** 249 (1991).
[3] Giovannozzi, M., Scandale, W., and Todesco, E., *Part. Accel.*, in press (1997).
[4] Warnock, R. L., and Ruth, R. D., *Physica D* **56** 188 (1992).
[5] Chao, A., *AIP Conf. Proc.* **230** 203 (1990).
[6] Yan, Y. *SSC* **500** (1991).
[7] Galluccio, F., and Schmidt, F., *Third European Particle Accelerator Conference* Gif sur Yvette: Edition Frontiéres (1993) pp. 640–42.
[8] Böge, M., and Schmidt, F., these proceedings.

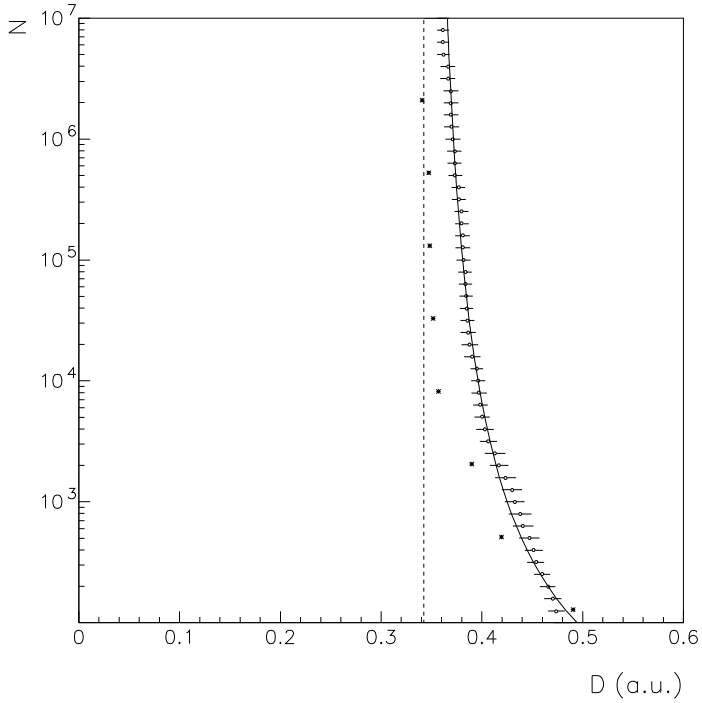

Figure 8: Dynamic aperture versus number of turns (dots) for the Hènon map at $\nu_x = 0.201$, $\nu_y = 0.112$; analytic interpolation (solid line) and extrapolation at infinity (dotted line). Prediction of the chaotic border according to the Lyapunov exponent (stars).

[9] Giovannozzi, M., Scandale, W., and Todesco, E., in preparation.
[10] Laskar, J., Froeschlé, C., and Celletti, A., *Physica D* **56** 253 (1992).
[11] Laskar, J., *Physica D* **67** 257 (1992).
[12] Bartolini, R., Bazzani, A., Giovannozzi, M., Scandale, W., and Todesco, E., *Part. Accel.* **52** 147 (1996).
[13] Bazzani, A., Bongini, S., and Turchetti, G., submitted to *Phys. Rev. E.*
[14] Todesco, E., Giovannozzi M., *Phys. Rev. E* **53** 4067 (1996).
[15] Hénon, M., and Heiles, C., *Astr. J.* **69-1** 73 (1964).
[16] Froeschlé, C., *Astron. & Astrophys.* **16** 172 (1972).
[17] Benettin, G., Galgani, L., Giorgilli, A., and Strelcyn, J. M., *Meccanica* **15-1** 21 (1980).
[18] Turchetti, G., private communication.
[19] Siegel, C. L., and Moser, J., *Lectures in celestial mechanics*, Berlin: Springer Verlag, 1971.
[20] Nekhoroshev, N., *Russ. Math. Surv.* **32** 1 (1977).
[21] Benettin, G., Galgani, L., Giorgilli, A., Servizi, G., and Turchetti, G., *Phys. Lett.* **95A** 11 (1983).
[22] Turchetti, G., *Number theory and physics* Berlin–Heidelberg: Springer Verlag 223 (1990).
[23] Bazzani, A., Marmi S., and Turchetti, G., *Cel. Mech.* **47** 333 (1990).
[24] Bazzani, A., and Turchetti, G., *Chaotic Dynamics: Theory and Practice* New York: Plenum Press 59 (1991).